Geochimica et Cosmochimica Acta, Vol. 69, No. 5, pp. 1145–1155, 2005
Copyright © 2005 Elsevier Ltd
Printed in the USA. All rights reserved
0016-7037/05 $30.00 + .00

doi:10.1016/j.gca.2004.08.014

Bioreduction of natural specular hematite under flow conditions

G. Gonzalez-Gil,[1,*] J. E. Amonette,[2] M. F. Romine,[2] Y. A. Gorby,[2] and G. G. Geesey[1]

[1]Department of Microbiology and Center for Biofilm Engineering, Montana State University, Bozeman, MT 59717, USA
[2]Pacific Northwest National Laboratory, Richland, WA 99352, USA

(*Received January* 23, 2004; *accepted in revised form August* 23, 2004)

Abstract—Dissimilatory reduction of Fe(III) by *Shewanella oneidensis* MR-1 was evaluated using natural specular hematite as sole electron acceptor in an open system under dynamic flow conditions to obtain a better understanding of biologic Fe(III) reduction in the natural environment. During initial exposure to hematite under advective flow conditions, cells exhibited a transient association with the mineral characterized by a rapid rate of attachment followed by a comparable rate of detachment before entering a phase of surface colonization that was slower but steadier than that observed initially. Accumulation of cells on the hematite surface was accompanied by the release of soluble Fe(II) into the aqueous phase when no precautions were taken to remove amorphous Fe(III) from the mineral surface before colonization. During the period of surface colonization following the detachment phase, cell yield was estimated at $1.5–4 \times 10^7$ cells/μmol Fe(II) produced, which is similar to that reported in studies conducted in closed systems. This yield does not take into account those cells that detached during this phase or the Fe(II) that remained associated with the hematite surface. Hematite reduction by the bacterium led to localized surface pitting and localized discrete areas where Fe (II) precipitation occurred. The cleavage plane of hematite left behind after bacterial reduction, as revealed by our results, strongly suggests, that heterogeneous energetics of the mineral surface play a strong role in this bioprocess. AQDS, an electron shuttle shown to stimulate bioreduction of Fe(III) in other studies, inhibited reduction of hematite by this bacterium under the dynamic flow conditions employed in the current study. *Copyright © 2005 Elsevier Ltd*

1. INTRODUCTION

Our current understanding of biologic iron (Fe) reduction is based primarily on studies of closed systems using soluble Fe(III) (Liu et al., 2001a, 2002; Haas and Dichristina, 2002) or synthetic Fe(III)-(hydr)oxides (Liu et al., 2001b; Benner et al., 2002; Doong and Schink, 2002; Nevin and Lovley, 2002a; Zachara et al., 2002; Roden, 2003). Natural environments likely to support biologic Fe reduction, however, typically are open systems and contain Fe(III) primarily in the form of crystalline (hydr)oxides such as hematite (α-Fe_2O_3) and goethite (α-FeOOH) (Bigham et al., 2002). Some dissimilatory Fe reducing bacteria (DIRB) have been shown to use these crystalline minerals as electron acceptors during anaerobic oxidation of organic matter (Zachara et al., 1998). However, the sustained long term reduction of crystalline Fe(III)-(hydr)oxides by DIRB remains to be demonstrated, and the reactions that control microbiologic Fe reduction are poorly understood, particularly under conditions of natural environments.

For sustained reduction of Fe(III)-(hydr)oxide, the electron transport system of some bacteria likely depends on access to the Fe(III)-(hydr)oxide surface and on the efficient displacement of the Fe(II) respiration product from that surface (Roden and Urrutia, 2002). It has been shown that soluble redox active substances such as natural humic material or synthetic compounds such as anthraquinone-2,6-disulfonate (ADQS) shuttle electrons between the respiratory apparatus of the bacterial cell and the solid phase Fe(III) (Lovley et al., 1996). Upon reduction by bacteria, these electron shuttling compounds diffuse to sites on the Fe(III)-(hydr)oxide surface, reduce the Fe(III) to Fe(II) and, in the process, become reoxidized and available to accept more electrons from the bacteria. Relatively small quantities of electron shuttling substances are required for reduction of Fe(III)-(hydr)oxides by some bacteria (Nevin and Lovley, 2000). In closed systems, the addition of soluble electron shuttles to cultures of DIRB has been shown to enhance rates of Fe(III)-(hydr)oxide reduction (Lovley et al., 1996). However, the effect of these shuttles on Fe(III)-(hydr)oxide reduction in flowing open systems has not been well studied.

At elevated soluble Fe(II) concentrations, the reduction of Fe(III) may become thermodynamically unfavorable (Kremer and Hering, 1997; Royer et al., 2002). Moreover, a portion of the Fe(II) produced during bioreduction of Fe(III)-(hydr)oxide sorbs either to the surface of the cell or to the Fe(III)-(hydr)oxide surface, impeding access of the cell to the solid-phase Fe(III) and thus inhibiting solid phase Fe(III) reduction (Roden and Zachara, 1996; Urrutia et al., 1998). Advective transport of Fe(II) has been suggested as one mechanism by which Fe(II)-mediated inhibition is alleviated (Roden and Urrutia, 1999; Roden et al., 2000; Roden and Urrutia, 2002).

Here we describe the reduction of specular hematite, a crystalline Fe(III) oxide having a macroscopic platy habit, by the dissimilatory Fe reducing bacterium *Shewanella oneidensis* MR-1. Our experiments were conducted in the presence and absence of the electron shuttle AQDS using a hydrodynamically-controlled, flow-through reactor. The open system represented by our approach should offer insight on bacterial reduction of solid phase Fe under conditions that simulate groundwater flow across mineral surfaces in the subsurface environment.

* Author to whom correspondence should be addressed, at Swiss Federal Institute of Technology (ETH) Zurich, Institute of Terrestrial Ecology, Grabenstrasse 3, CH-8952, Schlieren, Switzerland (gonzalez-gil@env.ethz.ch).

2. MATERIALS AND METHODS

2.1. Transformation of *Shewanella oneidensis* MR-1

Shewanella oneidensis MR-1 was transformed to constitutively express the gene (*gfp*) for Green Fluorescent Protein to facilitate detection of individual cells on opaque mineral surfaces by epifluorescence microscopy. Electrocompetent *S. oneidensis* MR-1 cells were prepared by growing cells at 30°C in Luria Broth (LB) to a final OD_{600} of 0.4, washing once with 1 mM HEPES (pH 7) and once with 20% glycerol. Cells were centrifuged at 5000 *g* for 20 min, and resuspended at a final concentration of $\sim 10^{10}$ cells/ml in 10% glycerol, and then aliquots of the cells were rapidly frozen in liquid nitrogen and stored at −80°C. Aliquots of electrocompetent *S. oneidensis* MR-1 cells were removed from −80°C storage and thawed on ice just before use. Plasmid p519ngfp (87453) was purchased from the American Type Culture Collection. Plasmid DNA (5–250 ng) was mixed with 100 μL of cells and incubated on ice for 5 min before transfer to a chilled (4°C) cuvette. The cuvette was quickly placed in a BioRad GenePulse unit and immediately electroporated at 750 V, 400 ohms and 25 μF. 250 μL of chilled (4°C) SOC medium (Sambrook and Russell, 2001) was immediately added to the cuvette and the cells quickly transferred to a 2 mL cryovial. The electroporated cells were allowed to recover at room temperature for 2 h on a rotating platform at 100 RPM. Transformants were selected on LB agar supplemented at 20 μg/ml with kanamycin and incubated at 30°C for 2–3 d. This transformant of *S. oneidensis* MR-1 carrying plasmid p519ngfp encoding kanamycin resistance and a constitutively expressing gene *gfp* is referred hereafter as *S. oneidensis GF*.

2.2. Cultivation of *S. oneidensis GF*

S. oneidensis GF was cultured routinely under static, anaerobic conditions in 160 mL serum bottles (sealed with butyl rubber septa and aluminum crimp caps) containing 100 mL of a defined liquid medium with a pH of 6.8–7.0. The medium prepared with distilled water contained (mM): NaH_2PO_4 (5), NH_4Cl (28), KCl (1.34), NaCl (0.17), $CaCl_2$ (0.68), $NaHCO_3$ (30), L-arginine (0.11), L-serine (0.20), L-glutamate (0.14), $MgSO_4$ (0.5), $MnSO_4$ (0.03), $CoSO_4$ (0.0064), $ZnSO_4$ (0.0062), $CuSO_4$ (0.0004), $KAl(SO_4)_2$ (0.0004), H_3BO_4 (0.0016), $NiCl_2$ (0.001), $FeCl_2$ (0.005), Na_2SeO_3 (0.0015), Na_2WO_4 (0.00075), Na_2MoO_4 (0.001). Lactate (43 mM) was added as electron donor. The medium in the bottles was made anaerobic by flushing with O_2-free N_2 gas, and the head space converted to an N_2:CO_2 mixture [80:20% (v/v)] before autoclave sterilization. Before inoculation, the medium was supplemented with the following filter sterilized components at the final concentrations shown: fumarate 35 mM (electron acceptor), kanamycin sulfate 100 mg/L (included to maintain selective pressure on the bacterial cells for retention of the plasmid and reporter gene), and vitamins solution 1 mL/L (Stams et al., 1992). A late exponential phase culture ($A_{660\ nm}$ 0.35) grown at 30°C in the above medium, but lacking $FeCl_2$, was used to inoculate the anaerobic flow cell reactors (AFC). $FeCl_2$ was omitted to avoid introduction of Fe(II) to the AFC.

2.3. Hematite Preparation

The specular hematite (α-Fe_2O_3) used in the AFCs was from Minas Gerais, Brazil, and kindly provided by Kevin M. Rosso, Pacific Northwest National Laboratory, Richland, WA. Unless noted otherwise, the hematite used in the experiments is unaltered. In several experiments however we used hematite treated with citrate-bicarbonate-dithionite (CBD) (van Oorschot and Dekkers, 1999) to remove surface-associated amorphous Fe, hereafter referred to as CBD-treated hematite.

2.4. Reactor Description and Preparation

The AFCs were constructed of Teflon with dimensions of 100 mm in length, 72 mm in width, and 14 mm in height (Fig. 1). AFCs had an internal flow channel 48 mm in length, 12 mm in width, and 0.8 mm in height. The floor of the channel contained two 2 mm-deep, depressions 1 cm in length and 1 cm in width to accommodate 1-cm^2 flakes of specular hematite, one surface of which was mounted flush with the channel floor. The ceiling of the flow channel consisted of a microscope cover glass viewing window (24 × 60 mm) sandwiched between a silicone rubber sheet and a Viton gasket that formed a leak-proof seal when overlaid with an aluminum cover plate that is tightened onto the Teflon housing with screws. Sterile culture medium, maintained in an anaerobic state by continuous purging with a mixture of N_2 and CO_2 (80:20% v/v), was delivered from a reservoir to the AFC. Medium delivery was under near pulse-free flow achieved using a reciprocating syringe pump (KDS210, KD Scientific, New Hope, PA) equipped with two 10-mL gas-tight syringes (SGE International, Australia). All tubing (1.016 mm internal diameter; 0.560 mm wall thickness), valves and fittings were of O_2 impermeable PEEK (Upchurch Scientific, Oak Harbor WA). The reactor system was assembled and then autoclave sterilized for 20 min. The syringes and valve components were submerged in water during sterilization to avoid damage due to pressure changes.

2.5. Reactor Operation

The sterile medium feed for the AFC was the same as that used for routine cultivation of the bacteria except that it was prepared with deionized water, fumarate and $FeCl_2$ were omitted, and the concentration of trace elements and amino acids were reduced by 50%. For some experiments the sterile medium feed was supplemented with the oxidized form of the redox-active compound, anthraquinone-2,6-disulfonate (AQDS) at a final concentration of 100 μM. Sterile anaerobic medium was first pumped from the medium reservoir through the sterile AFCs to remove gas bubbles, the AFCs were inoculated by pumping in the bacterial starter culture at a flow rate of 30 μL/min over a 4 h period, then the reactor feed was switched back to sterile medium and pumped through the AFCs at a flow rate of 30 μL/min for the duration of the experiment. An uninoculated AFC was operated in parallel with an inoculated AFC. In one experiment, an autoclave-sterilized culture was used as inoculum for the reactor to determine the effects of viable vs. nonviable biomass associated with the hematite surface on Fe reduction. All reactors were operated at room temperature (20 to 21°C), and experiments were performed in duplicate.

2.6. Analytical Methods

2.6.1. Fe(II)/Fe(III) determination

The AFC reactor effluent (5 mL) was collected directly into a tube containing ferrozine reagent (500 μL). The contents of the tube were centrifuged to sediment bacterial cells and the cell-free supernatant recovered for colorimetric analysis using the modified ferrozine method as described by Viollier et al. (2000). The Fe(II) concentration in each sample was determined from a standard curve in which absorbance was plotted against different Fe(II) concentrations introduced as ferrous ethylenediammonium sulfate. Matrix effects were accounted for using standard additions of known amounts of Fe(II) to subsamples. Separate 5-mL volumes of effluent were subjected to one of the following treatments: two subsamples were extracted for 1 h with 0.5 N HCl and one assayed directly and the other first centrifuged before assaying; two other subsamples were centrifuged or assayed directly without acid extraction. Since preliminary studies indicated that all treatments yielded similar Fe(II) concentrations, only soluble Fe from centrifuged, nonextracted subsamples are reported below.

2.6.2. Microscopy

Colonization of the hematite surfaces by *S. oneidensis GF* was evaluated nondestructively by direct microscopic examination without suspending flow. Microscopic examination and image video capture were as previously described (Neal et al., 2003). The density of cells on the mineral surface was determined by enumerating the number of GFP-fluorescing cells in microscopic images collected from 3 to 4 randomly chosen fields of view (400 μm^2) defined by an eyepiece graticule. Whereas dissolved O_2 is not required for the synthesis of GFP, it is required for GFP fluorescence. Since the dissolved O_2 concentration in the reactor was below the threshold required for GFP fluorescence (~1/300th the saturation concentration; Christensen et al., 1999; Hansen et al., 2001), a brief pulse (ca. 5 min) of aerobic, electron

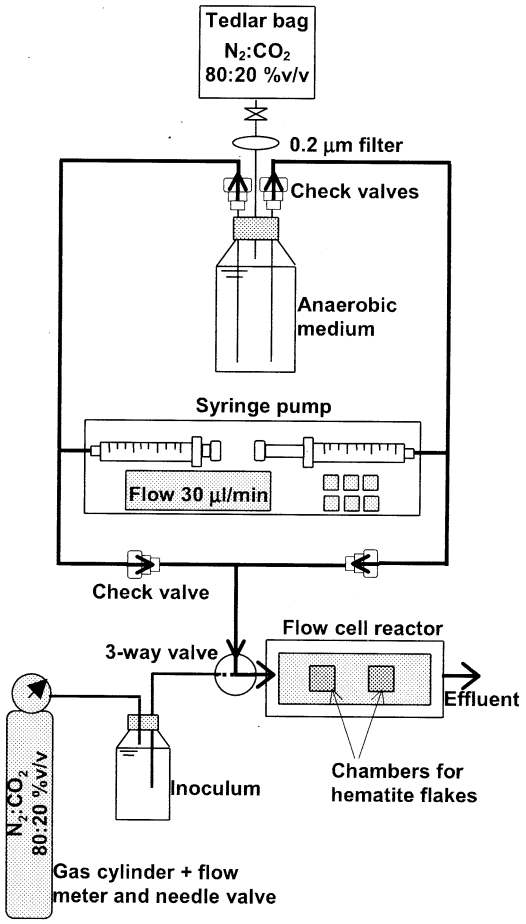

Fig. 1. Schematic of the anaerobic flow cell (AFC) reactor.

donor-free culture medium was introduced at 4, 288 and 680 h to the AFCs to induce fluorescence of GFP in cells 15 min before collection of an image.

2.6.3. X-ray photoelectron spectroscopy (XPS)

XPS was used to characterize the valence state of Fe at the hematite surface (McIntyre and Zetaruk, 1977). XPS spectra of the hematite surfaces were obtained with a Perkin Elmer 5600ci spectrometer (Perkin Elmer Inc., Eden Praire, MN) using a monochromatized AlK_α X-ray source (1486.6 eV) at 300 W. A pass energy of 46.95 eV and 23.50 eV was used for low and high resolution scans, respectively. The instrument was calibrated using the C*1s* photopeak, which has a binding energy of 284.8 eV. Spectra were obtained from a 4-mm^2 area of the hematite surface. Upon termination of an experiment, the AFCs were disconnected from the influent and effluent tubing and placed in an anaerobic chamber for disassembly and recovery of the hematite flakes. The hematite flakes were dried, mounted on stubs, and the stubs placed in N_2-purged, screwed-capped, plastic bottles during transfer from the anaerobic chamber to the anaerobic prechamber consisting of a N_2-purged plastic bag that was connected to the vacuum chamber of the XPS. By this procedure, the hematite flakes were maintained in an O_2-free atmosphere during transfer from the AFCs to the vacuum chamber of the XPS to avoid oxidation of hematite surface-associated Fe(II). The transfer processes from the prechamber to the XPS chamber took no more than 15 s.

2.6.4. Ag(I) reduction by reduced areas of hematite surface

High-resolution imaging of reduced areas of the hematite surfaces was carried out by reaction with dilute Ag(I) solutions and subsequent analysis using synchrotron X-ray microscopy (XRM) above the Ag K-edge as described by Amonette et al. (2003). Briefly, hematite flakes were recovered from the AFCs and rinsed with sterile, N_2-purged deionized water in an anaerobic chamber. The oxidant/fixative AgF_2(s) was dissolved in water and allowed to react overnight to produce 10 mM AgF/HF. Following overnight equilibration, the HF was neutralized (pH ~5.5) by addition of a slight excess of silicic acid (H_4SiO_4). After filtering through a 0.22-μm pore size membrane to remove any solids and sparging with N_2 this solution was reacted for 30 min with the surface of the hematite flakes in the anaerobic chamber. A different set of the hematite flakes exposed to similar conditions as those reacted with AgF/HF were exposed to a solution of 10 mM Ag acetate (CH_3COO^-) oxidant/fixative to avoid possible dissolution of precipitates formed on the hematite surface by HF. The Ag-reacted hematite flakes were then rinsed 3 times with sterile, N_2-sparged deionized water and dried before removing from the anaerobic chamber and mounting on glass slides using double-sided adhesive tape. The samples were stored under ambient conditions until analyzed by XRM. Hematite flakes exposed to 10 mM AgF/HF or Ag acetate but not bacteria were prepared as blanks.

2.6.5. Synchrotron X-ray microscopy (XRM)

XRM analysis was performed at beamline 20ID-B at the Advanced Photon Source, Argonne National Laboratory, Argonne, IL using incident photons of 26.0 keV energy. Kirkpatrick-Baez focusing optics (200-mm mirrors) and a 150-μm pinhole collimator were used to obtain a 9-μm^2 spot size taken normal to the beam axis. The specimens were oriented with the plane of the sample ~45° from the beam axis, and the 13-element Ge detector was normal to the beam axis (hence, 45° to the plane of the specimen). Spot size on the specimens, thus, was longer in the horizontal dimension than in the vertical dimension by a factor of 1.293, and step-size for sample movement in the horizontal direction was corrected by a factor of 0.707 to achieve uniform coverage of the sample. Spot size on the specimen surface was 13 μm^2. The integrated intensity of the K_α emission line of Ag was measured from the detector output using a multichannel analyzer. Step size was 5 μm and integration time per step was 0.5 s. Grayscale images of Ag(0) distribution and abundance in different areas of the hematite surface were prepared to display a range in intensity of 0 to 180,000 cts/pixel. Thus, intensities are quantitatively comparable in absolute terms across images.

3. RESULTS AND DISCUSSION

The colonization and reduction of natural specular hematite by *S. oneidensis GF* was examined under flow conditions in anaerobic AFC reactors. Reactors 1 and 2 (R1, R2) contained unaltered hematite flakes, while reactors 3 and 4 (R3, R4) contained CBD-treated hematite flakes. The effect of the electron shuttle AQDS was investigated by adding AQDS to the influent of R2 and R4.

3.1. Colonization of Hematite Surfaces by *S. oneidensis GF* under Continuous Flow Conditions

The use of strain *S. oneidensis GF*, which constitutively expresses GFP, permitted the detection and enumeration of this Fe-reducing bacterium on the planar surfaces of hematite (Fig. 2). Once synthesized, GFP remains stable within the cells until activated by O_2 to produce the fluorescent form of the protein (Tombolini et al., 1997). GFP fluorescence can be maintained in viable cells under anaerobic conditions for periods of time as long as ca. 900 h (Banning et al., 2002). Replicating cells can transfer their cytoplasmic pool of fluorescent GFP to daughter cells permitting visualization of several generations of cells that are never exposed to O_2 (Christensen et al., 1999). The colonization of *S. oneidensis GF* on

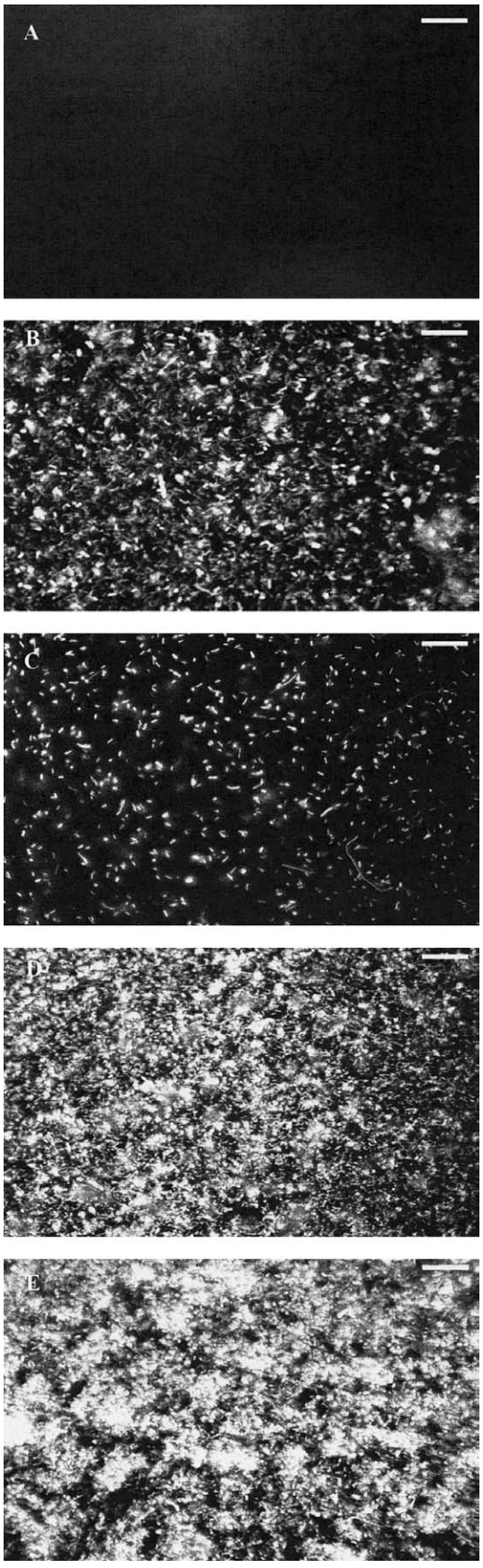

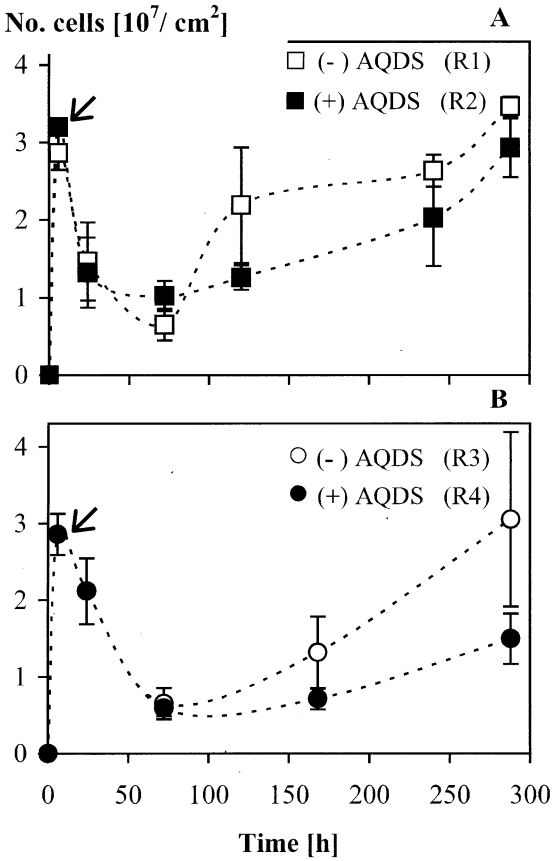

Fig. 3. Density of cells of *S. oneidensis GF* on hematite surfaces in AFC reactors during exposure to flowing anaerobic culture medium with and without AQDS. (A) Unaltered hematite was used in R1 and R2. (B) CBD-treated hematite was used in R3 and R4. The arrow indicates end of inoculation period (4 h after start of inoculation of AFCs).

hematite surfaces could be followed throughout the extended anaerobic experimental period (720 and 960 h) with only a limited pulse (5 min) of aerobic-electron free medium applied to the AFC reactors at time 4, 288 and 680 h of reactor operation.

S. oneidensis GF rapidly colonized the surface of hematite in the absence of AQDS (R1). The maximum cell density at the end of the 4-h inoculation phase of the AFC was 3.0×10^7 cells/cm^2 (Fig. 3A). The decrease in hematite surface-associated cell densities during the 25-h period following the switch of flow from inoculum to sterile medium, suggests that cells had detached from the surface during this period. ~75 h after AFC inoculation, cells began to accumulate again on the hematite surface (Fig. 3A). This increase in surface-associated cell densities indicates that cells were using solid phase Fe(III)

Fig. 2. Epifluorescence microscopic images of hematite surface during the colonization by *S. oneidensis GF* in the presence of flowing AQDS-free medium (R1). (A) Before reactor inoculation. (B) At 4 h after start of inoculation period immediately following initiation of flow of sterile culture medium. (C) At 72 h after inoculation. (D) At 288 h after inoculation. (E) At 680 h after inoculation. Bar = 10 μm.

to replicate on the hematite surface since no other source of alternative electron acceptor was present. The enumeration of cells was terminated 288 h following reactor inoculation since cell densities became too high to accurately determine by direct microscopic enumeration (Fig. 2). Colonization of hematite surfaces by *S. oneidensis GF* in the presence of 100 μM AQDS (R2) followed the same general pattern as that produced in the absence of AQDS (R1) (Fig. 3A). However, the rate of cell accumulation after the detachment phase was slower in the presence of AQDS than in the absence of AQDS.

When CBD-treated hematite was used in the AFC (R3,R4), colonization by *S. oneidensis GF* followed a similar trend as described above. Also the rate of cell accumulation on CBD-treated hematite after the detachment phase was slower in the presence of AQDS (R4) than in its absence (R3) (Fig. 3B).

In general, cells of *S. oneidensis GF* accumulated to a density of $\sim 3.0 \times 10^7$ cells/cm^2 on specular hematite after 288 h exposure to a flowing bulk aqueous phase that contained all of the nutrients required for cell growth except for the electron acceptor, which was supplied by the hematite (Fig. 3). This cell density is in the same order of magnitude as that reported for cells of *Shewanella alga* BrY (7.5×10^7 cells/cm^2), that had accumulated on synthetic hematite in a closed system (Das and Caccavo, 2001).

A yield of 1.5 to 4.0×10^7 cells/ μmol Fe(II) was obtained from the AFCs receiving AQDS-free medium. This estimate was based on 1) an exposed surface area of 1.5 cm^2 from microscopic area determinations performed with the image analysis software, 2) cell densities calculated from direct microscopic enumeration of cells associated with the exposed areas of hematite surface, and 3) the soluble Fe(II) measured in the reactor effluent (see next section) during the 72–288-h period following AFC inoculation. This yield should be viewed with caution, however, since it does not take into account the population of cells propagated on the surface that detached between periods of enumeration (Neal et al., 2003), or the amount of Fe(II) produced that remained associated with the hematite surface. Nevertheless, these values are similar in magnitude to the estimated $5–7 \times 10^7$ cells/μmol Fe(II) for growth of *S. oneidensis* MR-1 on clay minerals rich in Fe(III) (Kostka et al., 2002), and to the values of $\sim 4–9 \times 10^6$ cells/μmol Fe(II) during reduction of poorly crystalline Fe (hydr)oxide and goethite by other Fe reducing bacteria (Caccavo et al., 1992; Roden and Lovley, 1993).

3.2. Solubilization of Fe(III)

During the phase of cell accumulation on the hematite surfaces after the period of cell detachment, soluble Fe(II) was detected in the effluent of AFCs (R1) receiving AQDS-free medium (Fig. 4A). In contrast, no Fe(II) was detected in effluent of AFCs that 1) received only sterile anaerobic medium (i.e., uninoculated), 2) were inoculated with heat-killed cells, or 3) were inoculated with viable cells but exposed to anaerobic medium lacking lactate or any electron donor known to be used by *S. oneidensis* (data not shown). These results suggest that the Fe(II) in the effluent of R1 was produced as a result of respiration of the hematite-associated Fe(III) by hematite surface-associated cells. The concentration of Fe(II) in the effluent of R1 decreased from 2.5–3.0 μM to undetectable levels ($<$1 μM) between 200 and 670 h of reactor operation. In addition, no soluble Fe(III) was detected in the effluent of this reactor during the time that Fe(II) was detected (Fig. 4B).

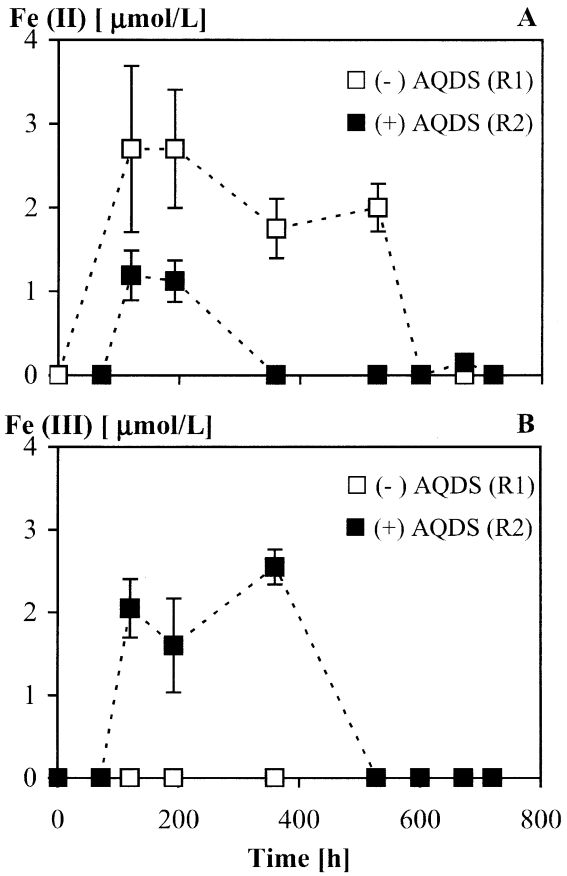

Fig. 4. Concentration over time of A) Fe(II) and B) Fe(III) in the effluent of inoculated AFCs containing unaltered hematite. AQDS at 100 μM was either absent (R1) or present (R2) in the influent anaerobic medium.

In contrast to the effluent of AFCs containing unaltered hematite (R1,R2), the effluent of AFCs with CBD-treated hematite (R3,R4) contained no detectable soluble Fe(II) or Fe(III), even though the AFCs were inoculated and operated under otherwise similar conditions (data not shown). These results suggest that the Fe(II) detected in the effluent of AFCs containing unaltered hematite was derived from bacterial reduction of amorphous Fe(III)-oxide associated with the hematite before exposure to bacteria in the AFCs. The decrease in the concentration of soluble Fe(II) in effluents of AFCs containing unaltered hematite (R1) 480 h following inoculation was therefore likely due to the depletion of the above mentioned amorphous Fe(III) (Fig. 4A). While this source of Fe(III) appears to have enhanced bacterial accumulation on hematite during the 75–150-h period following inoculation, it exerted no discernible influence on cell accumulation 288 h following inoculation (Figs. 3A,B).

The Fe(II) concentration in the effluent of AFCs (R2) receiving AQDS-containing medium was significantly less ($p < 0.05$) than in the AFCs (R1) lacking AQDS. Furthermore, soluble Fe(III), presumably in a complexed form, was detected in

effluent of AFCs (R2) receiving AQDS, but not in AFCs (R1) lacking AQDS (Fig. 4B). The effluent of uninoculated reactors fed with AQDS-containing medium, contained no detectable levels (detection limit 1 μM) of Fe(III) (data not shown), indicating that the Fe(III) was not solubilized through an abiotic reaction. Like that observed in AFCs (R1) the decrease in the concentration of soluble Fe(II) in the effluent of AFCs fed with AQDS-containing medium (R2) 380 h after inoculation was likely due to depletion of the above mentioned amorphous Fe(III) (Fig. 4A).

Based on the amount of soluble Fe(II) recovered in the effluent of R1 and R2, the bacteria appeared to reduce a very small fraction of hematite Fe(III) over the duration of the experiment. If one assumes an average effluent Fe(II) concentration of 2 μmol/L for the 670 h period during which Fe(II) was detected (Fig. 4A), at a reactor flow rate of 30 μL/min; then ~2.4 μmoles of hematite Fe(III) associated with the 1.5 cm^2 of exposed surface (0.001 m^2/g), or roughly 0.25% of the hematite in the reactor was reduced. Zachara et al. (1998) found that *Shewanella putrefaciens* CN32 reduced 0.6% of a synthetic powdered hematite with a surface area of 5.2 m^2/g. The lower conversion efficiency with specular hematite in our study is likely due, at least in part, to the smaller surface area accessible to the bacteria compared to that of the powdered hematite used by Zachara et al. (1998).

The soluble Fe(II) recovered in the effluent of the AFCs does not appear to reflect the Fe(III) reduction rates expected to support the accumulation of cells that was observed on the hematite surface. Whereas, the concentration of soluble Fe(II) in the effluent reached a plateau between 100 and 200 h following reactor inoculation, hematite surface-associated cell density continued to increase throughout the 288-h period following reactor inoculation in the presence or absence of AQDS. That soluble Fe(II) was not detected in effluents of AFCs R3 and R4, and did not increase in effluents of AFCs R1 and R2 during the period of cell accumulation on the hematite suggests that a portion of the Fe(III) reduced remained as an insoluble Fe(II) phase associated with the hematite surface. It is unlikely that a mobile, insoluble form of Fe(II) was released into the flowing bulk aqueous phase during this period, since preliminary studies showed no difference in the amount of Fe(II) recovered from the aqueous phase of subsamples acidified with 0.5 N HCl and those that received no acid treatment. Benner et al. (2002) and Hansel et al. (2003) found that significant quantities of secondary iron phases produced during bioreduction of ferrihydrite-coated sand remained associated with the solid phase under dynamic flow conditions. Rosso et al. (2003) detected nearly equimolar concentrations of aqueous Fe(II) and particle-associated Fe(II) during reduction of synthetic tabular hematite in a closed system.

3.3. Pitting of Hematite Surfaces

Reflected differential interference contrast (DIC) microscopy revealed a predominantly flat surface with some step edges of hematite growth faces, on unaltered hematite (AFCs R1, R2) and CBD-treated hematite (AFCs R3, R4) surfaces before inoculation of the AFCs with *S. oneidensis GF*. Since both surfaces displayed similar features, only those of CBD-treated hematite are presented (Fig. 5).

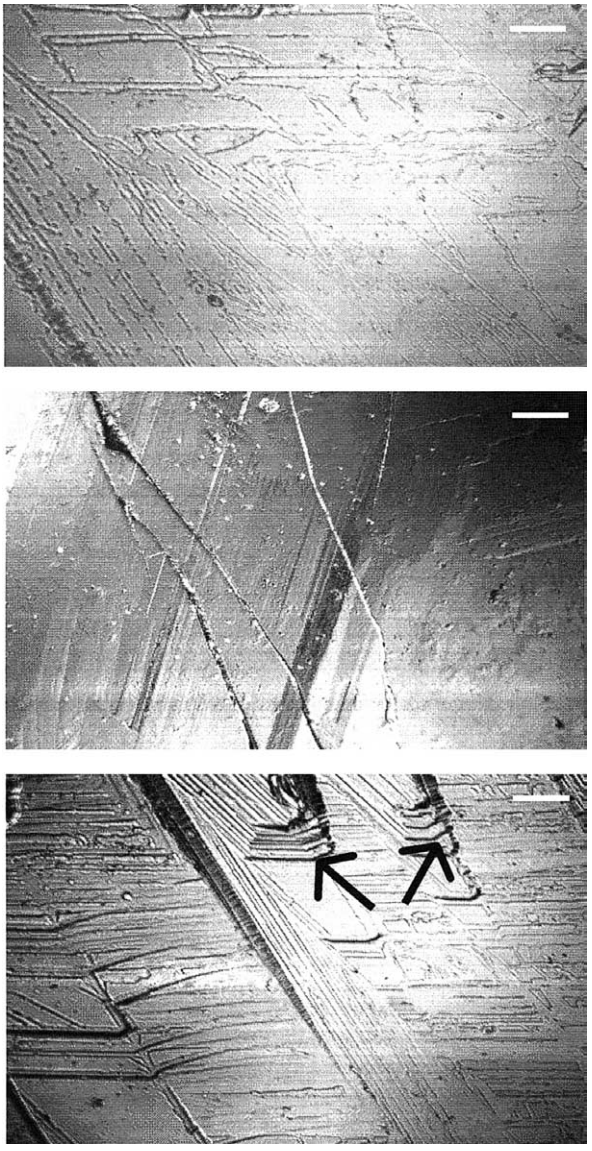

Fig. 5. Reflected DIC images of representative areas of the surface of CBD-treated hematite before installation in the AFC reactors. Arrows in bottom image show terraces of growth faces separated by step boundaries of the specular hematite. Bar = 10 μm.

Prominent surface pitting developed on the colonized hematite surfaces. In the absence of AQDS (R1) surface pitting was observed at 840 h after reactor inoculation. In the absence of AQDS, pitting was observed on CBD-treated hematite (R3) at 480 h. The pits increased in size over the period 480–960 h (Fig. 6). Pitting was also observed on hematite surfaces in AFCs (R2, R4) receiving AQDS-containing medium, although pitting was not as extensive as when AQDS was omitted. There was no evidence of surface pitting of hematite in AFCs, 1) that received only sterile anaerobic medium (i.e., uninoculated), 2) inoculated with heat-killed cells, or 3) inoculated with viable cells but exposed to anaerobic medium lacking electron donor (data not shown). This indicates that pitting requires the presence of active surface-associated bacterial cells. That pitting

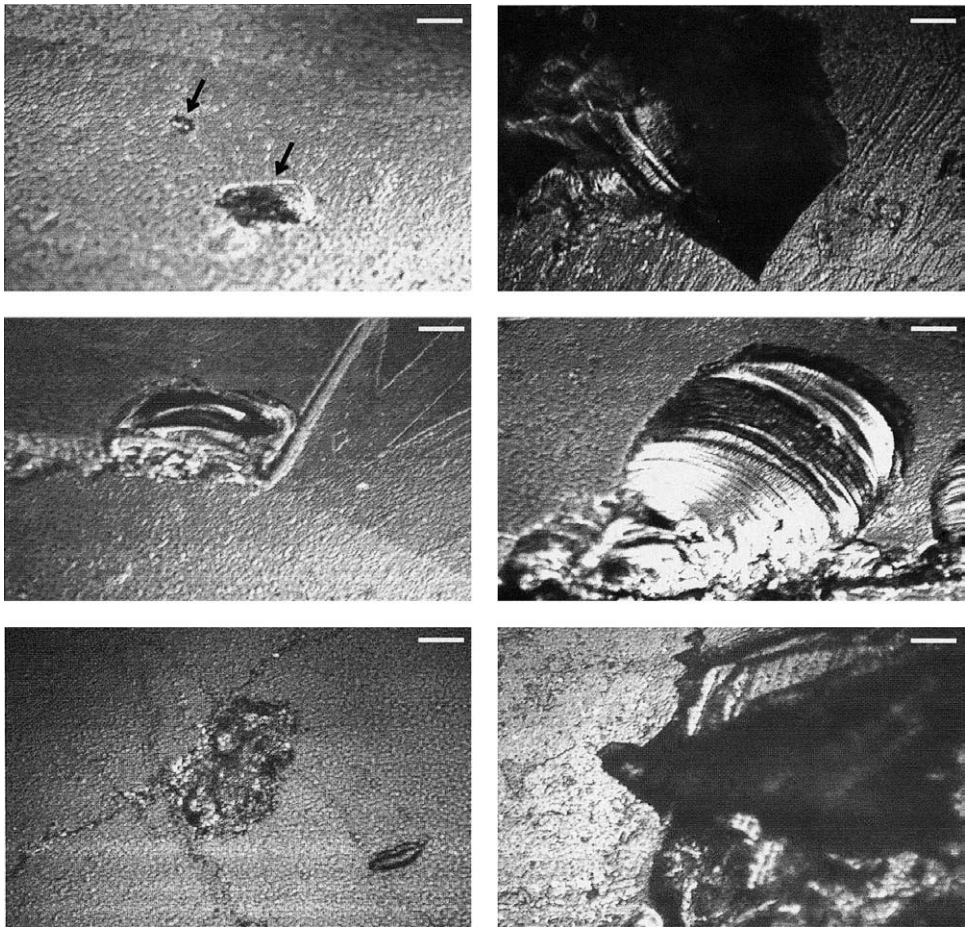

Fig. 6. Reflected DIC images of CBD-treated hematite after exposure to and colonization by cells of *S. oneidensis GF* in the presence of flowing AQDS-free culture medium (R3). Images on the left were obtained 480 h after AFC inoculation. Arrows in top left image show pits in early stage of development. Images on the right were obtained 960 h after AFC inoculation. Note evidence of enlargement of pits between 480 and 960 h. Bar = 10 μm.

occurred on CBD-treated hematite indicates that cells of *S. oneidensis GF* can solubilize crystalline Fe(III)-oxide.

Pits that appeared to be in early stages of development, most closely resembled the shallow etch pits randomly distributed across the flat terraces of synthetic tabular hematite colonized by cells of *Shewanella putrefaciens* CN32 in short-term batch studies (Rosso et al., 2003). In contrast to the nanometer-size pits described by these investigators, and the bacteria-size pits observed during bioreduction of microcrystalline oxyhydroxide coatings by cells of *S. putrifaciens* 200 (Grantham et al., 1997), our long-term (960 h) exposure studies without periodic reinoculation yielded pits that were tens of micrometers in diameter and presumably micrometers in depth, although depth profiles were not obtained in the present study. That none of these features were associated with the hematite surfaces exposed to conditions in which bioreduction was inhibited, supports these earlier observations that dissimilatory Fe(III) reduction of solid-phase minerals by some *Shewanella* spp. involves localized attack and dissolution of the solid phase (Grantham et al., 1997; Rosso et al., 2003). To our knowledge, this is the first report demonstrating that dissimilatory Fe(III) reduction of naturally-occurring, crystalline Fe(III)-oxides by this group of DIRB proceeds through localized attack and dissolution of the mineral surface. The exact mechanism of this localized attack as we observed in the AFCs is unknown, but may involve processes elucidated by Lower et al. (2001). By the use of atomic force microscopy, these authors show that under anaerobic conditions *S. oneidensis* rapidly develops strong adhesion energies at the interface with goethite. Following this mineral recognition event, *S. oneidensis* mobilizes and/or produces proteins that directly interact with the mineral surface (Lower et al., 2001).

3.4. XPS Characterization

The hematite surfaces were analyzed by XPS before inoculation, and at 240 h and 672 h of reactor operation. Similar Fe2*p* spectra were obtained for the hematite surface i) before inoculation (Fig. 7A), ii) 240 h after exposure to bacteria in the absence of AQDS (R1) (Fig. 7B), and iii) 240 h after exposure to sterile anaerobic medium (data not shown). The position and shape of the peak centered at 711 eV was similar to that reported for hematite surfaces (McIntyre and Zetaruk, 1977). The data suggest that for contact periods of 240 h or less, the

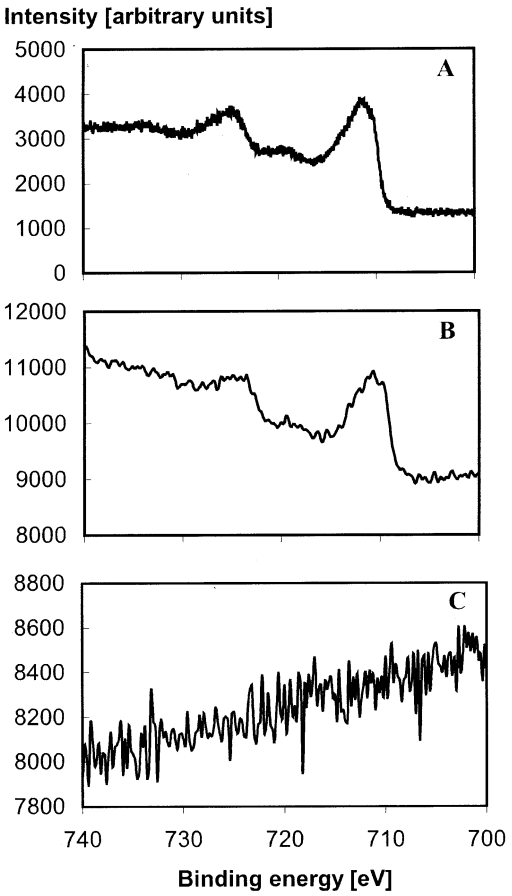

Fig. 7. Fe2*p* region of high resolution XP spectra of hematite surfaces from AFC (R1). (A) Before introduction to the AFC, (B) 240 h and (C) 672 h after AFC inoculation and exposure to flowing AQDS-free anaerobic culture medium.

impact of both the inoculated and the sterile treatments on those features of surface Fe chemistry resolvable by XPS was minimal. Moreover, surfaces exposed to bacteria for 672 h (R1) before analysis yielded spectra containing no useful information in the Fe2*p* region of the spectrum (Fig. 7C), presumably due to complete coverage of the hematite surface by bacterial cells.

The XP spectrum of the CBD-treated hematite surfaces before inoculation was similar to those produced by unaltered hematite surfaces before exposure to the bacteria (data not shown). Colonized, CBD-treated hematite surfaces were not evaluated by XPS based on the lack of useful Fe data obtained from the colonized unaltered hematite surfaces.

3.5. Reduction of CBD-Treated Hematite Surface

In view of the difficulty in detecting Fe(II) by XPS on the hematite surfaces, CBD-treated hematite surfaces were evaluated by XRM after 960 h of AFCs operation (R3,R4). The XRM technique involves treatment of the AFC sample with an aqueous solution containing Ag(I), which reacts with reduced species on the surface to precipitate Ag(0) particles. These particles are then detected by X-ray fluorescence using a synchrotron X-ray microprobe. In the present system, reduced species such as Fe(II) [the reduction potential at 25°C for the Ag^{+}/Ag (s) couple (+0.80 V) is just above that of the Fe^{3+}/Fe^{2+} couple (+0.77 V) (Stumm and Morgan, 1996)], and organic compounds associated with bacterial cells would yield

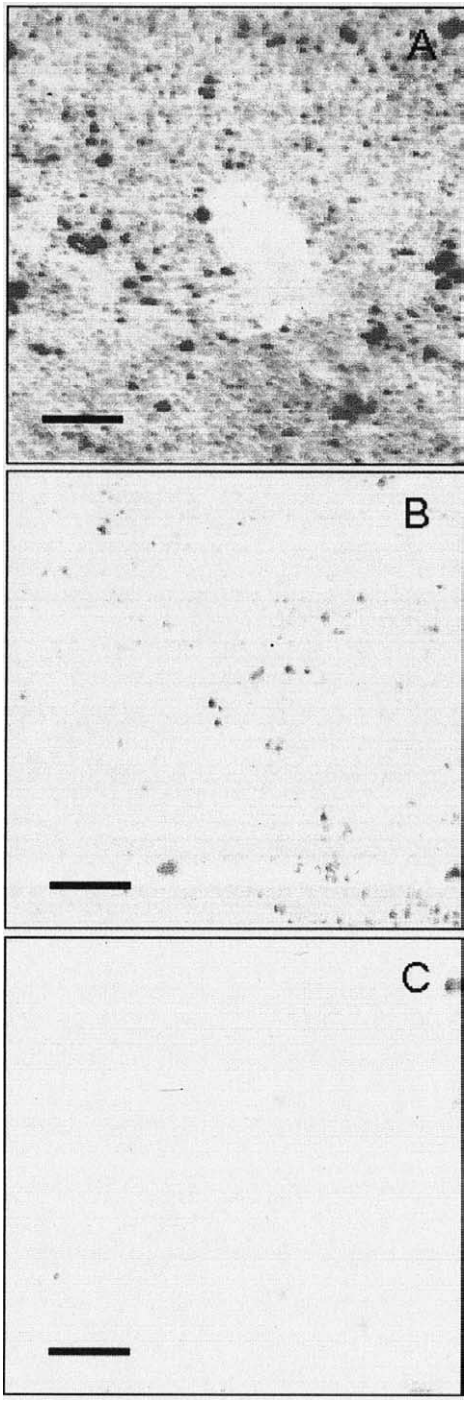

Fig. 8. Synchrotron XRM image of surface of CBD-treated hematite showing location of Ag-reducing areas 960 h after inoculation and exposure to flowing anaerobic (A) AQDS-free medium (AFC R3), (B) AQDS-containing medium (AFC R4), and (C) exposure to sterile flowing anaerobic medium only. Darker regions indicate greater Ag intensity. Bar = 100 μm.

Table 1. Mean values for Ag fluorescence observed by synchrotron XRM on the surfaces of CBD-treated hematite from AFC reactors after 960 h of operation.[a]

	Ag fluorescence (10^3 cts/pixel)		
	Anion		
AFC treatment	F^-	Acetate	Treatment means[b]
R3 Bacteria (− AQDS)	33[c]	14 (0)	21 (11)a
R4 Bacteria (+ AQDS)	10[c]	16 (5)	14 (5)a
Bacteria means	22(16)a	15 (3)a	17 (8)a
Sterile control	4[c]	7	6 (3)b

[a] The reactors were inoculated with *S. oneidensis GF* and fed with either AQDS-free (R3) or AQDS-containing (R4) anaerobic medium. Sterile control refers to uninoculated hematite.
[b] Treatment means followed by same letter in row or column are not significantly different at the $p < 0.05$ level.
[c] Single sample.

a Ag signal. XRM thus provides a means of determining the distribution and abundance of reactive Fe(II) and other reduced species at the hematite surface.

An abundance of discrete, micrometer-sized areas of Ag fluorescence (Fig. 8A, dark spots) were observed by XRM on AgF-reacted, CBD-treated, hematite surfaces colonized by *S. oneidensis GF* in the absence of AQDS (R3). A generally lower density of Ag fluorescence was observed under the same conditions when AQDS was present (R4) (Fig. 8B). As expected, little Ag fluorescence was observed for surfaces that had not been exposed to bacteria (Fig. 8C). For the Ag-acetate reacted, CBD-treated hematite surfaces colonized by the bacteria, a moderate density of Ag fluorescence was observed but no effect of AQDS was seen (images not shown).

Quantitatively, the amount of Ag measured on the AgF-reacted hematite surface colonized in the absence of AQDS (R3) was about three times larger than that measured for the surface colonized in the presence of AQDS (R4) (Table 1). Essentially no difference associated with AQDS was seen for the Ag-acetate reacted surfaces. As only a single replicate was analyzed for each of the AgF-treated surfaces, it is unclear the degree to which the Ag anion affected the analysis. Statistical analysis of the AQDS binomial treatment means showed no significant difference stemming from the presence or absence of AQDS. A significant difference, however, was observed with respect to the presence or absence of bacteria, with significantly ($p < 0.05$) higher Ag intensities observed for bacterially colonized surfaces (Table 1). Taken as a whole, the XRM data suggest that the impact of the electron shuttle compound AQDS was negligible with respect to the accumulation of Ag-reducible species [Fe(II)] on CBD-treated hematite surfaces containing biofilms of the Fe(III)-reducer *S. oneidensis GF*.

The XRM evidence of 2 to 8 times more Ag-reducible species on the surface area of CBD-treated hematite from colonized AFCs as compared to those from uncolonized AFCs exposed to sterile AQDS-containing or AQDS-free medium (Table 1), suggests that some Fe(II) produced during dissimilatory Fe(III) reduction remained associated with the hematite surface. Amonette et al. (2003) recently demonstrated that both abiotically and biotically generated reduced zones can be imaged on specular hematite using this approach, and that the amount of Ag observed on the surface of hematite correlated with the Fe(II) content of the surface precipitates and underlying mineral. Thus, more hematite was reduced by surface-associated cells of *S. oneidensis GF* under flowing conditions than indicated by the amount of soluble Fe(II) recovered in the effluent of the AFCs. The XRM images also show that the Fe precipitates were only localized suggesting that direct contact between the cell and the mineral was a key factor for hematite reduction.

3.6. Effect of AQDS on Bioreduction of Hematite Surfaces under Continuous Flow Conditions

AQDS has been reported to serve as an electron shuttle that enhances the reduction of soluble and insoluble crystalline and amorphous Fe(III) (hydr)oxides, primarily in closed experimental systems (Lovley et al., 1996; Fredrickson et al., 1998; Dong et al., 2003; Rosso et al., 2003). Few studies have evaluated the effect of AQDS on bioreduction of Fe(III) under flow conditions in open systems. Several different lines of evidence suggest that Fe(III) reduction by hematite surface-associated cells of *S. oneidensis GF* was inhibited, or at least, unaffected by AQDS under the conditions employed in the present study. First, lower concentrations of soluble Fe(II) were recovered in effluents of inoculated AFCs containing hematite when surface-associated bacteria were exposed to AQDS-containing medium compared to AQDS-free medium (Fig. 4A). Second, the rate of cell accumulation and maximum cell density achieved on CBD-treated hematite was considerable less in AFCs receiving AQDS-containing medium compared to that achieved in AFCs receiving AQDS-free medium over the 72–288-h period following AFC inoculation (Fig. 3). Third, pitting, an indicator of solubilization of Fe(III), which precedes reduction, was not as prevalent on hematite surfaces colonized by bacteria exposed to AQDS-containing medium compared to that achieved in AFCs receiving AQDS-free medium. Fourth, CBD-treated hematite surfaces colonized by bacteria exposed to AQDS-containing medium reduced the same or less Ag than surfaces colonized by bacteria exposed to AQDS-free medium.

In batch studies, AQDS has been shown to be less effective in promoting bioreduction of natural Fe(III)-oxides (0- to two-fold) than of synthetic Fe(III)-oxides (3- to 10-fold) (Zachara et al., 1998). Also, the AQDS enhancement effect on the bioreduction of powder hematite could only be observed during the first 24 h of incubation (Royer et al., 2002). It has been suggested that AQDS enhances bioreduction of some solid phase minerals by transferring electrons to Fe(III) present in micropores of the mineral not directly accessible to the bacteria (Hacherl et al., 2001). In the present study, bacteria were exposed primarily to a planar hematite surface, which likely contained fewer micropores than the mineral phases used in studies where the benefit of AQDS has been demonstrated. Additionally since AQDS is a dissolved component and can serve as electron acceptor by itself (Lovley et al., 1996; Newman and Kolter, 2000), it is possible that bacteria preferentially transferred the electrons to AQDS rather than to the hematite. Under continuous flow, a constant supply of AQDS might have shifted the role of this component from merely catalytic (aiding the reduction of iron minerals) to a principal role serving as main electron acceptor. Yet another point to consider, on why

no enhancement of Fe (III) reduction was observed in the presence of AQDS, is that the reduction of Fe (III) by reduced AQDS (i.e., anthrahydroquinone-2,6-disulfonate, AH_2QDS) might be rate limiting. To our knowledge, there are no studies to document the kinetic behavior of abiotic reductive dissolution of Fe(III)-(hydr)oxides by AH_2QDS.

The observation that AQDS promoted the release of Fe(III) (R2) from hematite into the flowing aqueous medium is difficult to interpret. Soluble Fe(III) has been reported in sediment pore waters and ground waters (4–16 μM) as well as in incubations of rice paddy soils (20–25 μM) where Fe(III) reduction is favored (Nevin and Lovley, 2002b and references therein). Under the conditions of this study, AQDS may transfer electrons from Fe(II) back to a soluble form of Fe(III), which is subsequently displaced from the hematite surface and removed from the Fe(III) reduction zone by advective flow. The extent to which AQDS controls the relative proportions of soluble Fe(III) and Fe(II), and the significance of soluble Fe(III) in Fe (III)-reducing environments needs further investigation.

4. CONCLUDING REMARKS

In the present study we employed an open, anaerobic, flow-through reactor system to evaluate dissimilatory bioreduction of a naturally-occurring crystalline phase Fe(III)-(hydr)oxide (hematite), to better understand the process under conditions that approach those of subsurface environments. Specifically, bulk aqueous phase chemistry and hydrodynamics at the bulk aqueous phase/mineral surface interface can be controlled better through the experimental system described here than in closed systems. Accumulation of cells was accompanied by the release of soluble Fe(II) into the aqueous phase when no precautions were taken to remove amorphous Fe(III) from the mineral surface before colonization. Colonization of hematite surfaces by *S. oneidensis GF* led to localized surface pitting and the establishment of discrete areas on the surface that could reduce Ag(I), possibly sites of Fe(II) precipitation. In contrast to previous reports documenting the stimulatory effect of AQDS on bioreduction of Fe(III), the electron shuttle appeared to inhibit bioreduction of hematite under the experimental conditions employed here. Further studies are needed to understand why open experimental systems yield results that, in some instances, differ from those obtained in closed systems.

Acknowledgments—This work was supported by the U.S. Department of Energy, Office of Science, Natural and Accelerated Bioremediation Research (NABIR) program by grants DE-FG03-98ER62630/A001 and DE-FG03-01ER63270 to Washington State University. We thank the anonymous reviewers and Dr. J Amend for their critical and insightful comments.

Associate editor: J. P. Amend

REFERENCES

Amonette J. E., Heald S. M., and Russell C. K. (2003) Imaging the heterogeneity of mineral surface reactivity using Ag(I) and synchrotron X-ray microscopy. *Phys. Chem. Miner.* **30,** 559–569.

Banning N., Toze S., and Mee B. J. (2002) *Escherichia coli* survival in groundwater and effluent measured using a combination of propidium iodide and the green fluorescent protein. *J. Appl. Microbiol.* **93,** 69–76.

Benner S. G., Hansel C. M., Wielinga B. W., Barber T. M., and Fendorf S. (2002) Reductive dissolution of iron hydroxide under dynamic flow conditions. *Environ. Sci. Technol.* **36,** 1705–1711.

Bigham J. M., Fitzpatrick R. W., and Schulze D. G. (2002) Iron oxides. In *Soil Mineralogy with Environmental Applications* (eds. J. B. Dixon and D. G. Schulze). Soil Science Society of America, pp 323–366.

Caccavo F., Blakemore R. P., and Lovley D. R. (1992) A hydrogen-oxidizing, Fe(III)-reducing microorganism from the Great Bay Estuary, New Hampshire. *Appl. Environ. Microbiol.* **58,** 3211–3216.

Christensen B. B., Sternberg C., Andersen J. B., Palmer R. J., Nielsen A. T., Givskov M., and Molin S. (1999) Molecular tools for study of biofilm physiology. *Methods Enzymol.* **310,** 20–42.

Das A. and Caccavo F. (2001) Adhesion of dissimilatory Fe(III)-reducing bacterium *Shewanella alga* BrY to crystalline Fe (III) oxides. *Curr. Microbiol.* **42,** 151–154.

Dong H., Kukkadapu R. K., Fredrickson J. K., Zachara J. M., Kennedy D. W., and Kostandarithes H. M. (2003) Microbial reduction of structural Fe(III) illite and goethite. *Environ. Sci. Technol.* **37,** 1268–1276.

Doong R. A. and Schink B. (2002) Cysteine-mediated reductive dissolution of poorly crystalline iron(III) oxides by Geobacter sulfurreducens. *Environ. Sci. Technol.* **36,** 2939–2945.

Fredrickson J. K., Zachara J. M., Kennedy D. W., Dong H., Onstott T. C., Hinman N. W., and Li S.-M. (1998) Biogenic iron mineralization accompanying the dissimilatory reduction of hydrous ferric oxide by a groundwater bacterium. *Gechim. Cosmochim. Acta* **62,** 3239–3257.

Grantham M. C., Dove P. M., and DiChristina T. J. (1997) Microbially catalyzed dissolution of iron and aluminum oxyhydroxide mineral surface coatings. *Geochim. Cosmochim. Acta* **21,** 4467–4477.

Hacherl E. L., Kosson D. S., Young L. Y., and Cowan R. M. (2001) Measurement of iron (III) bioavailability in pure iron oxide minerals and soils using anthraquinone-2,6 disulfonate oxidation. *Environ. Sci. Technol.* **35,** 4886–4893.

Hansel C. M., Benner S. G., Neiss J., Dohnalkova A., Kukkadapu R. K., and Fendorf S. (2003) Secondary mineralization pathways induced by dissimilatory iron reduction of ferrihydrite under advective flow. *Geochim. Cosmochim. Acta* **67,** 2977–2992.

Hansen M. C., Palmer R. J., Udsen C., White D. C., and Molin S. (2001) Assessment of GFP fluorescence in cells of *Streptococcus gordonii* under conditions of low pH and low oxygen concentration. *Microbiology.* **147,** 1383–1391.

Haas J. R. and Dichristina T. J. (2002) Effects of Fe(III) chemical speciation on dissimilatory Fe(III) reduction by *Shewanella putrefaciens. Environ. Sci. Technol.* **36,** 373–380.

Kostka J. E., Dalton D. D., Skelton H., Dollhopf S., and Stucki J. W. (2002) Growth of iron (III)-reducing bacteria on clay minerals as the sole electron acceptor and comparison of growth yields on a variety of oxidized iron forms. *Appl. Environ. Microbiol.* **68,** 6256–6262.

Kremer S. M. and Hering J. G. (1997) Influence of solution saturation state on the kinetics of ligand-controlled dissolution of oxide phases. *Geochem. Cosmochim. Acta* **61,** 2855–2866.

Liu C., Zachara J. M., Gorby Y. A., Szecsody J. E., and Brown C. F. (2001a) Microbial reduction of Fe(III) and sorption/precipitation of Fe (II) on *Shewanella putrefaciens* strain CN32. *Environ. Sci. Tech.* **35,** 1385–1393.

Liu C., Kota S., Zachara J. M., Fredrickson J. K., and Brinkman C. K. (2001b) Kinetic analysis of the bacterial reduction of goethite. *Environ. Sci. Technol.* **35,** 2482–2490.

Liu C., Gorby Y. A., Zachara J. M., Fredrickson J. K., Brown C. F. (2002) Reduction kinetics of Fe(III), Co(III), U(VI), Cr(VI) and Tc(VII) in cultures of dissimilatory metal-reducing bacteria. *Biotechnol. Bioeng*. **80,** 637–649.

Lovley D. R., Coates J. D., Blunt-Harris E. L., Phillips E. J. P., and Woodward J. C. (1996) Humic substances as electron acceptors for microbial respiration. *Nature* **382,** 445–448.

Lower S. K., Hochella M. F., Jr., and Beveridge T. J. (2001) Bacterial recognition of mineral surfaces: Nanoscale interactions between *Shewanella* and α-FeOOH. *Science* **292,** 1360–1363.

McIntyre N. S. and Zetaruk D. G. (1977) X-ray photoelectron spectroscopic studies of iron oxides. *Anal. Chem.* **49,** 1521–1529.

Neal A. L., Rosso K. M., Geesey G. G., Gorby Y. A., Little B. J. (2003) Surface structure effects on direct reduction of iron oxides by *Shewanella oneidensis. Geochim. Cosmochim. Acta* **67,** 4489–4503.

Nevin K. P. and Lovley D. R. (2000) Potential for nonenzymatic reduction of Fe(III) via electron shuttling in subsurface sediments. *Environ. Sci. Technol.* **34,** 2472–2478.

Nevin K. P. and Lovley D. R. (2002a) Mechanisms for accessing insoluble Fe (III) oxide during dissimilatory Fe(III) reduction by *Geothrix fermentans. Appl. Environ. Microbiol.* **68,** 2294–2299.

Nevin K. P. and Lovely D. R. (2002b) Mechanisms for Fe(III) oxide reduction in sedimentary environments. *Geomicrobiol. J.* **19,** 141–159.

Newman D. K. and Kolter R. (2000) A role for excreted quinones in extracellular electron transfer. *Nature* **405,** 94–97.

Roden E. E. (2003) Fe(III) oxide reactivity toward biological versus chemical reduction. *Environ. Sci. Technol.* **37,** 1319–1324.

Roden E. E. and Lovley D. R. (1993) Dissimilatory Fe(III) reduction by the marine microorganism Desulfuromonas acetoxidans. *Appl. Environ. Microbiol.* **59,** 734–742.

Roden E. E. and Urrutia M. M. (1999) Ferrous iron removal promotes microbial reduction of crystalline iron (III) oxides. *Environ. Sci. Technol.* **33,** 1847–1853.

Roden E. E., Urrutia M. M., and Mann C. J. (2000) Bacterial reductive dissolution of crystalline Fe (III) oxide in continuous-flow column reactors. *Appl. Environ. Microbiol.* **66,** 1062–1065.

Roden E. E. and Urrutia M. M. (2002) Influence of biogenic Fe (II) on bacterial crystalline Fe (III) oxide reduction. *Geomicrobiol. J.* **19,** 209–251.

Roden E. E. and Zachara J. M. (1996) Microbial reduction of crystalline Fe(III) oxides: influence of oxide surface area and potential for cell growth. *Environ. Sci. Technol.* **30,** 1618–1628.

Royer R. A., Burgos W. D., Fisher A. S., Jeon B. H., Unz R. F., and Dempsey B. A. (2002) Enhancement of hematite bioreduction by natural organic matter. *Environ. Sci. Technol.* **36,** 2897–2904.

Rosso K. M., Zachara J. M., Fredrickson J. K., Gorby Y. A., and Smith S. C. (2003) Nonlocal bacterial electron transfer to hematite surfaces. *Geochim. Cosmochim. Acta* **67,** 1081–1087.

Sambrook J. and Russell D. W. (2001) *Molecular Cloning*. Vol. 3, 3rd ed. Cold Springs Harbor Laboratory Press.

Stams A. J. M., Grolle K. C. F., Frijters C. T. M. J., and van Lier J. B. (1992) Enrichment of thermophilic propionate-oxidizing bacteria in syntrophy with *Methanobacterium thermoautotrophicum* or *Methanobacterium thermoformicicum*. *Appl. Environ. Microbiol*. **58,** 346–352.

Stumm W. and Morgan J. J. (1996) *Aquatic Chemistry: Chemical Equilibria and Rates in Natural Waters*. 3rd ed Wiley.

Tombolini R., Unge A., Davey M. E., de Bruijin F. J., and Jansson J. K. (1997) Flow citometry and microscopic analysis of GFP-tagged *Pseudomonas fluorescens* bacteria. *FEMS Microbiol. Ecol*. **22,** 17–28.

Urrutia M. M., Roden E. E., Fredrickson J. K., and Zachara J. M. (1998) Microbial and geochemical controls on synthetic Fe(III) oxide reduction by *Shewanella alga* strain BrY. *Geomicrobiol. J.* **15,** 269–291.

van Oorschot I. H. M. and Dekkers M. J. (1999) Dissolution behavior of fine-grained magnetite and maghemite in the citrate-bicarbonate-dithionite extraction method. *Earth Planet. Sci. Lett*. **167,** 283–295.

Viollier E., Inglett P. W., Hunter K., Roychoudhyry A. N., and Van Cappellen P. (2000) The ferrozine method revisited: Fe(II)/Fe(III) determination in natural waters. *Appl. Geochem.* **15,** 785–790.

Zachara J. M., Fredrickson J. K., Li S-M., Kennedy D. W., Smith S. C., and Gassman P. L. (1998) Bacterial reduction of crystalline Fe^{3+} oxides in single phase suspensions and subsurface materials. *Am. Mineral.* **83,** 1426–1443.

Zachara J. M., Kukkadapu R. K., Fredrickson J. K., Gorby Y. A., and Smith S. C. (2002) Biomineralization of poorly crystalline Fe(III) oxides by dissimilatory metal reducing bacteria (DMRB). *Geomicrobiol. J.* **19,** 179–207.